# A6 HEXAGONAL SILICON CARBIDE (2H-, 4H-, and 6H-SiC)

## A6.1 GENERAL REMARKS

Of all the polytypes, 6H is by far the most commonly occurring modification in commercial SiC. The next most common polytypes are 15R and 4H, respectively. SiC also crystallizes in the wurtzite structure (2H-SiC). Assuming that the 3C and 2H structures are extremes in the parameter describing the percentage of hexagonal close packing (often called *hexagonality*) with 0 and 100%, respectively, we get the hexagonal nature of 33% for 6H structure, 40% for 15R structure, and 50% for 4H structure. The hexagonal and rhombohedral polytypes have a sixhold symmetry axis along the stacking direction (*c* axis), and thus these crystals present an anisotropic (uniaxial) behavior of physical properties.

## A6.2 ELECTRONIC ENERGY-BAND STRUCTURE

Figure A6-1 shows the electronic energy-band structures of (a) 2H-SiC, (b) 4H-SiC, and (c) 6H-SiC as obtained within the DFT-LDA calculations by Käckell *et al.* [1]. The polytypes, 2H–6H, consist of identical layers, whose stacking sequences differ, and can be regarded as natural superlattices (4H- and 6H-SiC). The artificial semiconductor superlattices, like Si/Ge and GaAs/AlGaAs suprelattices, are characterized by band folding, band offset, and carrier confinement. We note, however, that the band offset is absent in 4H- and 6H-SiC. This is because there is no interface effect on the charge density and thus the stacking layer cannot be actually distinguished. As a result, no carrier-confinement effect is expected in 4H- and 6H-SiC. Only the band-folding effect is, therefore, important in this type of superlattices.

The hexagonal SiC polytypes are all indirect-band-gap semiconductors. The valence-band maximum at the Γ point is split into a twofold and a onefold state by hexagonal crystal field. The conduction-band minimum located at the X point in 3C-SiC changes to the L–M line in 6H or at the M point in 4H, and then to the K point in 2H-SiC. However, in the 6H-SiC its exact position on the L–M line is under discussion (see Refs. [2,3]). We summarize in Table A6-1 the lowest-indirect-exciton gaps obtained experimentally for some hexagonal and rhombohedral SiC polytypes [4], together with their corresponding hexagonalities. It can be seen from this table that the lowest indirect gap increases with increasing hexagonality. This famous relationship had been found in 1964 by Choyke, Hamilton, and Patrick [5,6].

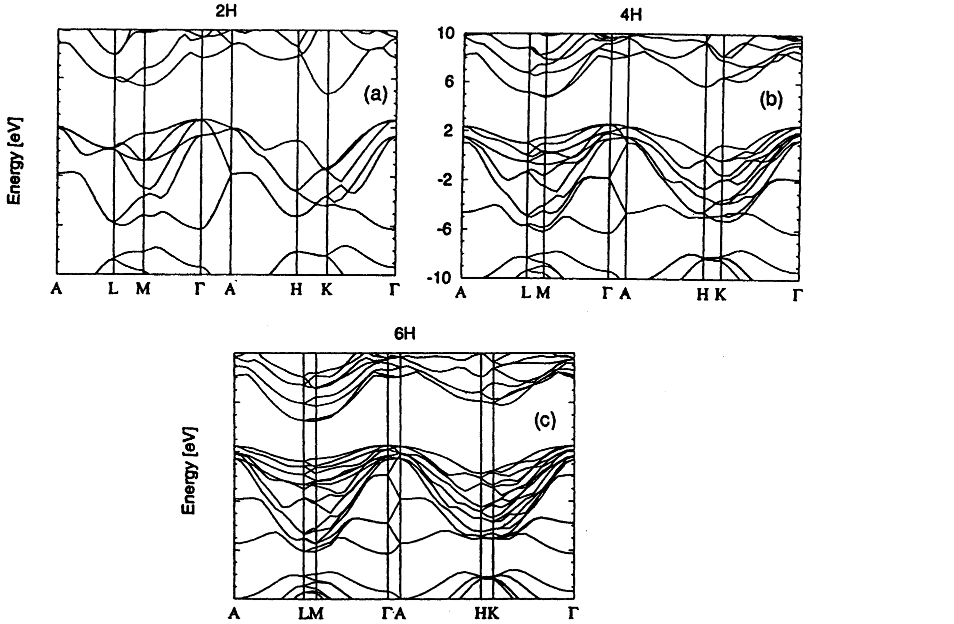


**Figure A6-1** Electronic energy-band structures of (a) 2H-SiC, (b) 4H-SiC, and (c) 6H-SiC as obtained within the DFT-LDA calculations. (From Käckell *et al.* [1].)

**TABLE A6-1** *Lowest-indirect-exciton gap and hexagonality for some SiC polytypes.*

| Polytype | Exciton Gap (eV) | Hexagonality (%) |
|---|---|---|
| 3C | 2.390 | 0 |
| 24R | 2.728 | 25 |
| 8H | 2.80 | 25 |
| 21R | 2.853 | 29 |
| 6H | 3.023 | 33 |
| 15R | 2.986 | 40 |
| 4H | 3.265 | 50 |
| 2H | 3.330 | 100 |

Figure A6-2 shows the theoretical reflectivity spectra for 2H-, 4H-, 6H-, and 3C-SiC polytypes as calculated by Lambrecht *et al.* [7]. The band structures were calculated by means of the scalar-relativistic LMTO method. The imaginary part of the dielectric function $\varepsilon_2(E)$ was derived at the random-phase approximation level using the muffin-tin-orbital basis set. The real part $\varepsilon_1(E)$ was then obtained from $\varepsilon_2(E)$ by means of the KK transformation. No lifetime broadening effect was taken into consideration in the calculation. The experimental data for 4H, 15R, 6H, and 3C polytypes measured by these authors are also shown in Fig. A6-2 by the solid lines.

In Fig. A6-2, the overall experimental features are broader than the theoretical

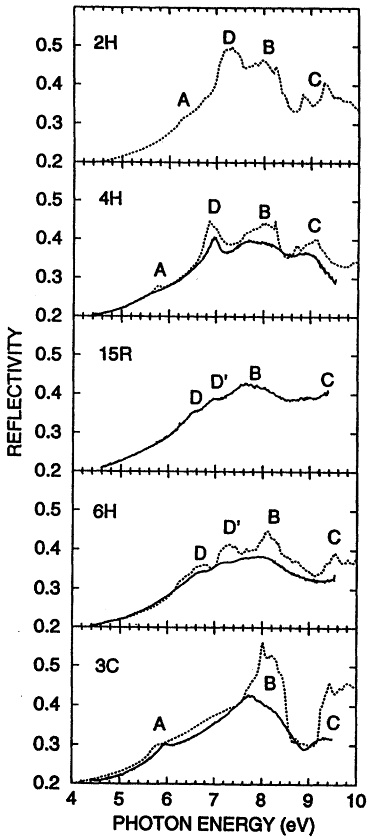


**Figure A6-2** Reflectivity spectra for 2H-, 4H-, 15R-, 6H-, and 3C-SiC polytypes: dotted lines (theory), solid lines (experiment at 300 K). The data for 2H-, 4H-, 15R-, and 6H-SiC correspond to $\boldsymbol{E}\perp c$. Note that no lifetime broadening effect was taken into consideration in the theory. (From Lambrecht *et al.* [7].)

ones. Nevertheless, a clear correspondence can be established between all main features in the experiment and calculation. The main peak of 3C-SiC ($B$) is centered at 7.8 eV (see also Fig. A5-5). A peak near 8 eV exists in all polytypes considered. It is flattened out in 4H and 6H and shifted to slightly lower energy in 15R. It is considered to mostly correspond to transitions from the upper two valence bands to the lowest conduction band ($E_0$ or $E_1$) in the case of 3C-SiC and to similar transitions of the appropriately folded bands in the smaller BZs of the hexagonal polytypes. A second peak ($C$) appears at higher energy in the calculated spectra of all polytypes. In 3C-SiC, this peak may correspond to transitions from the upper valence band to the second conduction band ($E_0'$, $E_1'$, or $E_2'$).

The main difference between the cubic and all other polytypes consists of the features ($D$, $D'$) centered near 7 eV. This feature is strongest in 2H, sharpest in 4H, split into two peaks ($D$, $D'$) in both 15R and 6H, and absent in 3C. The peak $D$ in 2H-SiC was found to correspond to an extended region of the nearly parallel band in the Γ–K–X plane near K [7]. Similar flat interband-transition curves also exist in 4H and 6H along the Γ–K line. This axis of the hexagonal BZ corresponds to the Σ=Γ–K and Q=L–W lines of cubic SiC which are both folded onto the T=Γ–K line of the hexagonal BZ.

## A6.3 OPTICAL CONSTANTS

*(a) 2H-SiC* —There are very few reports on the optical constants of 2H- and 4H-SiC polytypes [7-10]. Powell [8] reported the $n$ data for 2H-SiC measured by the method of minimum deviation over the wavelength range 435.8–650.9 nm. The crystals used were grown by the reduction of methyltrichlorosilane ($CH_3SiCl_3$) at 1375°C. They were in the form of needles about 0.4 mm in diameter by 2 mm long, and their $c$ axis was in the direction of the needle's length. A curve fit of the measured $n$ data to the Cauchy dispersion equation

$$n = A + \frac{B}{\lambda^2} + \frac{C}{\lambda^4} \qquad \text{(A6.1)}$$

yielded $A$=2.5513, $B$=2.585×10$^4$, and $C$=8.928×10$^8$ for the ordinary ray ($E \perp c$) and $A$=2.6161, $B$=2.823×10$^4$, and $C$=11.490×10$^8$ for the extraordinary ray ($E \| c$) when $\lambda$ is expressed in nm. The $n$ data for 2H-SiC, together with those for 3C-, 4H-, 6H-, and 15R-SiC, are plotted in Fig. A6-3 [8].

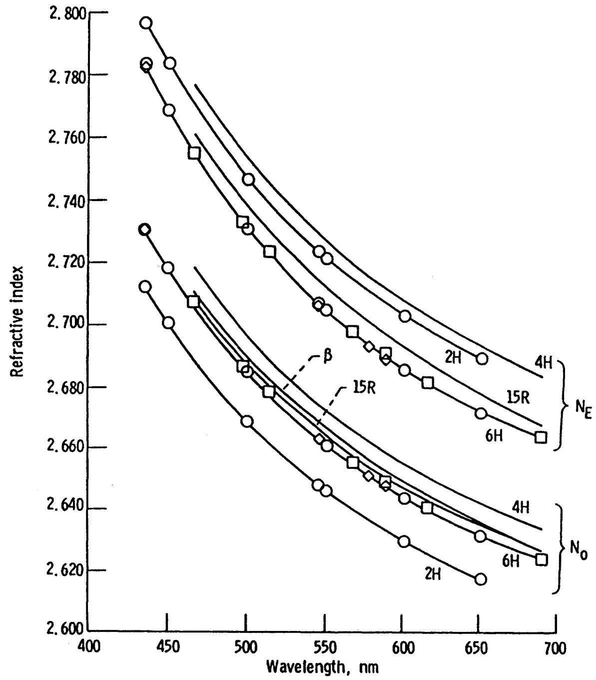


**Figure A6-3** Refractive-index dispersion for SiC polytypes. Data included for 2H and 6H curves only. The 3C (β), 4H, and 15R curves are from Shaffer [9]. Diamonds, Thibault (see Ref. [8]); squares, Shaffer [9]; circles, Powell [8]. (From Powell [8].)

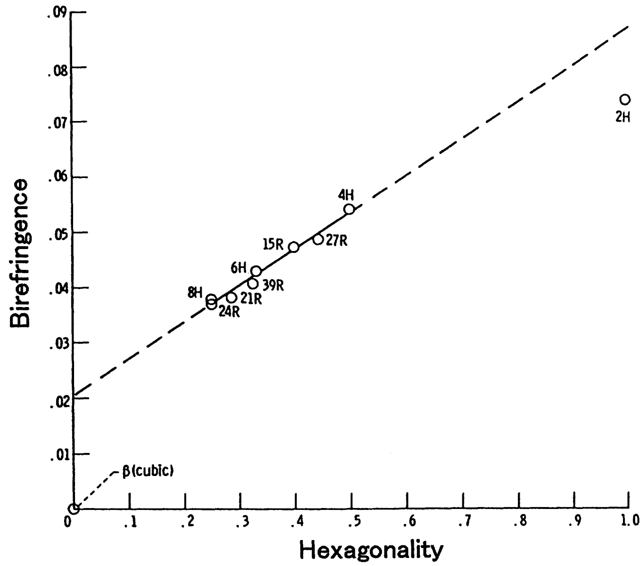


**Figure A6-4** Birefringence vs. hexagonality for SiC polytypes at λ=584 nm. (From Powell [8].)

Figure A6-4 plots the birefringence, $\Delta n \equiv n_e(\boldsymbol{E} \parallel c) - n_o(\boldsymbol{E} \perp c)$, vs. hexagonal fraction (hexagonality) for some SiC polytypes at 584 nm [8]. There have been attempts to relate the birefringence of SiC to the crystal structure [8,9,11]. In the structurally analogous system of ZnS polytypes, the birefringence is a linear function of the hexagonal fraction $h$ [12]. The situation for SiC is not so simple. As seen in Fig. A6-4, the birefringence is a linear function of $h$ for values of $h$ between 0.25 and 0.50. However, the values for 3C-SiC ($h$=0) and 2H-SiC ($h$=1.0) are considerably below this line.

We list in Table A6-2 the $\varepsilon_1$, $n$, and $R$ [$=(n-1)^2/(n+1)^2$] values for 2H-SiC. They were calculated from Eq. (A6.1) [8]. Limiting $\lambda \to \infty$ in Eq. (A6.1), we obtain the high-frequency dielectric constant $\varepsilon_\infty$=6.51 for $\boldsymbol{E} \perp c$ and 6.84 for $\boldsymbol{E} \parallel c$.

**Table A6-2** *Optical constants of 2H-SiC at 300 K.*

| eV | $\boldsymbol{E} \perp c$ $\varepsilon_1$ | $n$ | $R$ | $\boldsymbol{E} \parallel c$ $\varepsilon_1$ | $n$ | $R$ |
|---|---|---|---|---|---|---|
| 1.904 | 6.8503 | 2.6173 | 0.200 | 7.2318 | 2.6892 | 0.210 |
| 2.061 | 6.9143 | 2.6295 | 0.202 | 7.3057 | 2.7029 | 0.211 |
| 2.249 | 7.0018 | 2.6461 | 0.204 | 7.4066 | 2.7215 | 0.214 |
| 2.270 | 7.0119 | 2.6480 | 0.204 | 7.4185 | 2.7237 | 0.214 |
| 2.476 | 7.1214 | 2.6686 | 0.207 | 7.5460 | 2.7470 | 0.217 |
| 2.753 | 7.2927 | 2.7005 | 0.211 | 7.7468 | 2.7833 | 0.222 |
| 2.844 | 7.3555 | 2.7121 | 0.213 | 7.8210 | 2.7966 | 0.224 |

***(b) 4H-SiC***—The $n$ dispersion data for 4H-SiC were reported by Shaffer [9] (see Figs. A6-3 and A6-4). The crystals were grown by the sublimation method. The experimental $n$ data were fitted to the Cauchy dispersion formula of Eq. (A6.1) with $C$=0. The fit-determined dispersion parameters were: $A$=2.5610 and $B$=3.40×10$^4$ for $E \perp c$; $A$=2.6041 and $B$=3.75×10$^4$ for $E \| c$.

Biedermann [10] studied the optical absorption properties of some SiC polytypes, including 4H-SiC, in the wavelength range 0.35 to 2.5 μm with light polarization perpendicular and parallel to the $c$ axis. He observed in N-doped $n$-type samples ($n$~5×10$^{18}$ cm$^{-3}$) the main absorption bands in the 0.6–3-eV region that were strongly dependent upon the polytype and light polarization. These bands were assumed to be due to electron excitation from the conduction-band minimum to other sites of increased DOS in the higher, empty band (namely, due to the intracondution-band absorption). No comparable absorption bands were observed in Al-doped, $p$-type samples. The absorption coefficients in the $p$-type samples increased continually from the minimum near the band edge towards longer wavelengths, the dependence being given approximately by $k \sim \lambda^{1.5}$ for the ordinary ray and $k \sim \lambda^{0.9}$ for the extraordinary ray.

Sridhara *et al.* [13] have also reported the absorption coefficients of 4H-SiC measured at 300 K, with light propagating along the $c$ axis, from 3900 to 3350 Å. The sample was $n$ type with an impurity concentration in the high 10$^{14}$ cm$^{-3}$. It was carefully polished to a thickness of 64 μm. By using the known shift of the band gap with temperature, they have also given the absorption values at 2 K.

The fundamental reflectivity spectrum in the interband transition region of 4H-SiC was reported by Lambrecht *et al.* [7] (see Fig. A6-2). We note, however, that the reflectivity peak value at ~7 eV for 3C-SiC obtained by these authors is considerably smaller than the recent SE result (cf. Fig. A5-5).

More recently, Zollner and Hilifker [14] have reported the SE $\varepsilon(E)$ spectra of 4H-SiC from 0.72 to 6.6 eV. The sample studied was obtained commercially from Cree Research. It was not intentionally doped and single-side polished (Si-terminated). The sample was measured as received without surface preparation. The SE data revealed CP near 5.53 eV.

Table A6-3 lists the optical-constant data for 4H-SiC. They were obtained for $E \leq 2.654$ eV from Shaffer [9] and for $E \geq 3$ eV from Zollner and Hilifker [14]. These data yield the high-frequency dielectric constants $\varepsilon_\infty$=6.56 for $E \perp c$ and 6.78 for $E \| c$ [$\lambda \rightarrow \infty$ in Eq. (A6.1)].

**Table A6-3** *Optical constants of 4H-SiC at 300 K.*

| | $E \perp c$ | | | | | $E \| c$ | | |
|---|---|---|---|---|---|---|---|---|
| eV | $\varepsilon_1$ | $\varepsilon_2$ | $n$ | $k$ | $R$ | $\varepsilon_1$ | $n$ | $R$ |
| 1.794 | 6.9353 | | 2.6335 | | 0.202 | 7.2006 | 2.6834 | 0.209 |
| 2.012 | 7.0267 | | 2.6508 | | 0.204 | 7.3078 | 2.7033 | 0.212 |
| 2.104 | 7.0692 | | 2.6588 | | 0.206 | 7.3544 | 2.7119 | 0.213 |
| 2.182 | 7.1049 | | 2.6655 | | 0.206 | 7.3940 | 2.7192 | 0.214 |

**Table A6-3** *Continued (4H-SiC).*

| | $E\perp c$ | | | | | $E\parallel c$ | | |
|---|---|---|---|---|---|---|---|---|
| eV | $\varepsilon_1$ | $\varepsilon_2$ | $n$ | $k$ | $R$ | $\varepsilon_1$ | $n$ | $R$ |
| 2.407 | 7.2259 | | 2.6881 | | 0.210 | 7.5350 | 2.7450 | 0.217 |
| 2.489 | 7.2792 | | 2.6980 | | 0.211 | 7.5889 | 2.7548 | 0.218 |
| 2.654 | 7.3908 | | 2.7186 | | 0.214 | 7.7123 | 2.7771 | 0.221 |
| 3 | 7.59 | | 2.75 | | | | | |
| 3.1 | 7.68 | | 2.77 | | | | | |
| 3.2 | 7.70 | | 2.77 | | | | | |
| 3.3 | 7.87 | | 2.81 | | | | | |
| 3.4 | 7.98 | | 2.82 | | | | | |
| 3.5 | 8.10 | 0.01 | 2.85 | 0.0018 | 0.996 | | | |
| 3.6 | 8.22 | 0.02 | 2.87 | 0.0035 | 0.991 | | | |
| 3.7 | 8.36 | 0.03 | 2.89 | 0.0052 | 0.987 | | | |
| 3.8 | 8.50 | 0.04 | 2.92 | 0.0069 | 0.983 | | | |
| 3.9 | 8.65 | 0.05 | 2.94 | 0.0085 | 0.979 | | | |
| 4 | 8.81 | 0.08 | 2.97 | 0.013 | 0.968 | | | |
| 4.1 | 8.99 | 0.09 | 3.00 | 0.015 | 0.965 | | | |
| 4.2 | 9.18 | 0.12 | 3.03 | 0.020 | 0.954 | | | |
| 4.3 | 9.40 | 0.14 | 3.07 | 0.023 | 0.948 | | | |
| 4.4 | 9.62 | 0.19 | 3.10 | 0.031 | 0.931 | | | |
| 4.5 | 9.87 | 0.23 | 3.14 | 0.037 | 0.919 | | | |
| 4.6 | 10.1 | 0.31 | 3.18 | 0.049 | 0.895 | | | |
| 4.7 | 10.4 | 0.35 | 3.23 | 0.054 | 0.885 | | | |
| 4.8 | 10.7 | 0.45 | 3.27 | 0.069 | 0.859 | | | |
| 4.9 | 11.1 | 0.54 | 3.33 | 0.081 | 0.840 | | | |
| 5 | 11.4 | 0.68 | 3.38 | 0.101 | 0.809 | | | |
| 5.1 | 11.8 | 0.80 | 3.44 | 0.116 | 0.787 | | | |
| 5.2 | 12.3 | 0.96 | 3.51 | 0.137 | 0.762 | | | |
| 5.3 | 12.8 | 1.19 | 3.58 | 0.166 | 0.730 | | | |
| 5.4 | 13.4 | 1.53 | 3.67 | 0.209 | 0.692 | | | |
| 5.5 | 13.9 | 2.08 | 3.74 | 0.278 | 0.645 | | | |
| 5.6 | 14.4 | 2.73 | 3.81 | 0.358 | 0.616 | | | |
| 5.7 | 14.7 | 3.24 | 3.86 | 0.420 | 0.606 | | | |
| 5.8 | 15.2 | 3.78 | 3.93 | 0.481 | 0.605 | | | |
| 5.9 | 15.6 | 4.41 | 3.99 | 0.553 | 0.610 | | | |
| 6 | 16.1 | 5.10 | 4.06 | 0.628 | 0.620 | | | |
| 6.1 | 16.6 | 5.92 | 4.14 | 0.716 | 0.636 | | | |
| 6.2 | 17.3 | 6.87 | 4.24 | 0.811 | 0.656 | | | |
| 6.3 | 17.8 | 8.25 | 4.33 | 0.954 | 0.684 | | | |
| 6.4 | 18.3 | 9.69 | 4.42 | 1.10 | 0.710 | | | |
| 6.5 | 18.6 | 11.3 | 4.49 | 1.26 | 0.736 | | | |

*(c) 6H-SiC*—The reported $\varepsilon_\infty$ data for 6H-SiC have yielded widely different values ranging from 6.17 to 6.7 for $E\perp c$ and from 6.49 to 6.72 for $E\parallel c$ [15]. Pikhtin *et al.* [16] measured the $n$ data in the 0.4–50-μm wavelength region at 297 and 105 K and estimated from their data the static and high-frequency dielectric constants to be $\varepsilon_s$=9.66 (9.64) and $\varepsilon_\infty$=6.520 (6.509) for $E\perp c$ and $\varepsilon_s$=10.09 (10.01) and $\varepsilon_\infty$=6.742 (6.692) for $E\parallel c$ at 297 K (105 K).

IR optical properties of 6H-SiC have been studied by Spitzer *et al.* [17] and more recently by Engerlbrecht and Helbig [18]. The samples used by Engerlbrecht and Helbig [18] were cut from boules grown by a modified Lely method ($n$=0.5–1.0×$10^{17}$ $cm^{-3}$). The measured spectra were fitted to the classical Lorentz oscillator model. The number of the Lorentz oscillators required for this fit was one for $\boldsymbol{E}\perp c$ and five for $\boldsymbol{E}\| c$: four extra oscillators for $\boldsymbol{E}\| c$ correspond to two weak one-phonon absorption lines in the reststrahlen band and two weak absorption lines at longer wavelengths. Spitzer *et al.* [17] reported additional, but only *one* weak absorption line in the reststrahlen band for $\boldsymbol{E}\| c$. The reststrahlen data of Engerlbrecht and Helbig [18] yielded the $\varepsilon_\infty$ values of 6.17 and 6.49 for $\boldsymbol{E}\perp c$ and $\boldsymbol{E}\| c$, respectively, while Spitzer *et al.* [17] obtained the $\varepsilon_\infty$ value of 6.7 both for $\boldsymbol{E}\perp c$ and $\boldsymbol{E}\| c$.

The $n$ dispersion in 6H-SiC has been studied by many authors [8,9,16,19,20]. Like 2H- and 4H-SiC, the ordinary values $n_o$ ($\boldsymbol{E}\perp c$) are usually smaller than the extraordinary ones $n_e$ ($\boldsymbol{E}\| c$) at the same wavelengths (i.e., $\Delta n=n_e-n_o>0$, see Fig. A6-3).

Optical absorption at the fundamental absorption edge of 6H-SiC has been studied by a number of authors [21–5]. The data revealed fine structures caused by phonons involved in the indirect-transition process [23].

Optical absorption in the region well below the fundamental absorption edge has been studied by Biederman [10] and Ellis and Moss [26]. These authors observed the relatively strong absorption peaks at $E$~1.6 eV in the $n$-type samples for $\boldsymbol{E}\| c$. Their peak strengths were found to increase with increasing carrier concentration [26]. They were considered to arise from the interconduction-band absorption [10]. It was also found [26] that the absorption edge for $\boldsymbol{E}\perp c$ occurs at slightly longer wavelength than that for $\boldsymbol{E}\| c$, in agreement with the data of Choyke and Patrick [23]. The free-carrier absorption, however, showed no evidence of anisotropy in the scattering mechanism [26].

Fundamental reflectivity study in the interband transition region of 6H-SiC was performed by Lambrecht *et al.* [7] in the 4–9.5-eV region (see Fig. A6-2), by Philipp and Taft [27] in the 1–11.5-eV region, and by Wheeler [28] in the 3–13-eV region. Unfortunately, the Refs. [7] and [28] authors did not performed KK analysis. Philipp and Taft [27] performed KK analysis, but they did not state whether the data were measured for $\boldsymbol{E}\perp c$, or $\boldsymbol{E}\| c$, or a mixture.

The SE data for 6H-SiC have been reported by Adachi and coworker [15] in the 1.2–5.4-eV region for both $\boldsymbol{E}\perp c$ and $\boldsymbol{E}\| c$ and more recently by Logothetidis and Petalas [29] in the 1.5–9.5-eV region for $\boldsymbol{E}\perp c$. The measured SE data showed CP features at energies ~6.7 and 9.2 eV for $\boldsymbol{E}\perp c$ [29] and at ~5.4 eV for $\boldsymbol{E}\| c$ [15]. Logothetidis and Petalas [29] also found that the $n$ dispersion for $\boldsymbol{E}\perp c$ below the lowest-direct-band gap (1.5–5.5 eV) can be fitted by the Sellmeier equation:

$$\varepsilon_1(\lambda) = n(\lambda)^2 = 1.0 + \sum_i \frac{A_i\lambda^2}{\lambda^2 - \lambda_{0i}{}^2} \qquad \text{(A6.2)}$$

with $A_1$=1.481, $\lambda_{01}$=0.1817 μm, $A_2$=4.142, and $\lambda_{02}$=0.1597 μm. Adachi and coworker [15] also reported the fitted results of their measured $n$ data for $\boldsymbol{E}\perp c$ and $\boldsymbol{E}\| c$ using the first-order Sellmeier equation.

More recently, Zollner and Hilifker [14] have measured the $\varepsilon(E)$ spectra of 6H-SiC from 0.72 to 6.6 eV using rotating-analyzer ellipsometer. The sample was obtained commercially from Cree Research. It was not intentionally doped and single-side polished (Si-terminated). The sample was measured as received without surface preparation. The accuracy for $\varepsilon_2$ was reported to be 0.01.

The optical constants in the UV–soft X-ray region (10.2–525 eV) of SiC were reported by Windt *et al.* [30]. The samples used by them were grown by CVD. The Si *L* absorption edge was visible in the extinction coefficient near 100 eV. The dip in the *n* dispersion near 21 eV was also found.

Tables A6-4 and A6-5 list the room-temperature values of $\varepsilon=\varepsilon_1+i\varepsilon_2$, $n^*=n+ik$, $\alpha$, and *R* for 6H-SiC for $\boldsymbol{E}\perp c$ and $\boldsymbol{E}\parallel c$, respectively. A set of the optical constants for $E\leq0.12$ eV for $\boldsymbol{E}\perp c$ ($E\leq0.22$ eV for $\boldsymbol{E}\parallel c$) were calculated using the reststrahlen parameters in Ref. [18]. [Note that in Table III of Ref. [18], the values of $\Gamma_i/\omega_i$ (not $\Gamma_i$) were listed.] The $k$ ($\alpha$) values in the region $0.14\leq E\leq2.3$ eV ($0.24\leq E\leq2.4$ eV) for $\boldsymbol{E}\perp c$ ($\boldsymbol{E}\parallel c$) were taken from Ellis and Moss [26] ($n=1.11\times10^{17}$ cm$^{-3}$). Some optical constants for $0.14\leq E\leq2.3$ eV for $\boldsymbol{E}\perp c$ were taken from Refs. [18] and [29], while those for $0.24\leq E\leq2.4$ eV for $\boldsymbol{E}\parallel c$ were taken from Refs. [15] and [18]. A complete set of the optical constants in the region $2.5\leq E\leq9.5$ eV for $\boldsymbol{E}\perp c$ were taken from Logothetidis and Petalas [29], and those above 2.5 eV for $\boldsymbol{E}\parallel c$ were taken from Ref. [15]. The optical constants above 10.2 eV for $\boldsymbol{E}\perp c$ were taken from Windt *et al.* [30].

The ($\varepsilon_1$, $\varepsilon_2$), ($n$, $k$), $\alpha$, and *R* values in Tables A6-4 and A6-5 are graphed in Figs. A6-5–A6-8, respectively. The solid and dashed lines represent the data for $\boldsymbol{E}\perp c$ and $\boldsymbol{E}\parallel c$, respectively.

## REFERENCES


1. P. Käckell, B. Wenzien, and F. Bechstedt, *Phys. Rev. B* **50**, 10761 (1994).
2. C. H. Park, B.-H. Cheng, K.-H. Lee, and K. J. Chang, *Phys. Rev. B* **49**, 4485 (1994).
3. B. Wenzien, P. Käckell, F. Bechstedt, and G. Gappellini, *Phys. Rev. B* **52**, 10897 (1995).
4. *Numerical Data and Functional Relationships in Science and Technology*, edited by K.-H. Hellwege and O. Madelung, Landolt–Börnstein, New Series, Group III, Vol. 17, Pt. a (Springer, Berlin, 1982).
5. W. J. Choyke, D. R. Hamilton, and L. Patrick, *Phys. Rev.* **133**, A1163 (1964).
6. L. Patrick, D. R. Hamilton, and W. J. Choyke, *Phys. Rev.* **143**, 526 (1966).
7. W. R. L. Lambrecht, B. Segall, M. Yoganathan, W. Suttrop, R. P. Devaty, W. J. Choyke, J. A. Edmond, J. A. Powell, and M. Alouani, *Phys. Rev. B* **50**, 10722 (1994).
8. J. A. Powell, *J. Opt. Soc. Am.* **62**, 341 (1972).
9. P. T. B. Shaffer, *Appl. Opt.* **10**, 1034 (1971).

10. E. Biedermann, *Solid State Commun.* **3**, 343 (1965).
11. Yu. A. Makhalov and E. N. Mokhov, *Sov. Phys. Solid State* **18**, 1451 (1976).
12. O. Brafman and I. T. Steinberger, *Phys. Rev.* **143**, 501 (1966).
13. S. G. Sridhara, R. P. Devaty, and W. J. Choyke, *J. Appl. Phys.* **84**, 2963 (1988).
14. S. Zollner and J. N. Hilifker, *Phys. Status Solidi A* **166**, R9 (1998).
15. S. Ninomiya and S. Adachi, *Jpn. J. Appl. Phys.* **33**, 2479 (1994).
16. A. N. Pikhtin, V. T. Prokopenko, V. S. Rondarev, and A. D. Yas'kov, *Opt. Spectrosc.* **43**, 420 (1977).
17. W. G. Spitzer, D. Kleinman, and D. Walsh, *Phys. Rev.* **113**, 127 (1959).
18. F. Engelbrecht and R. Helbig, *Phys. Rev. B* **48**, 15698 (1993).
19. W. J. Choyke and L. Patrick, *J. Opt. Soc. Am.* **58**, 377 (1968).
20. V. B. Bogdanov, A. N. Pikhtin, V. F. Tsvetkov, and A. D. Yas'kov, *Opt. Spectrosc.* **52**, 644 (1982).
21. H. R. Philipp, *Phys. Rev.* **111**, 440 (1958).
22. R. Groth and E. Kauer, *Phys. Status Solidi* **1**, 445 (1961).
23. W. J. Choyke and L. Patrick, *Phys. Rev.* **127**, 1868 (1962).
24. W. J. Choyke and L. Patrick, *Phys. Rev.* **172**, 769 (1968).
25. V. V. Makarov, *Sov. Phys.–Semicond.* **6**, 1556 (1973).
26. B. Ellis and T. S. Moss, *Proc. Roy. Soc. A* **299**, 393 (1967).
27. H. R. Philipp and E. A. Taft, in *Silicon Carbide–A High Temperature Semiconductor*, edited by J. R. O'Connor and J. Smiltens (Pergamon, Oxford, 1960), p. 366.
28. B. E. Wheeler, *Solid State Commun.* **4**, 173 (1966).
29. S. Logothetidis and J. Petalas, *J. Appl. Phys.* **80**, 1768 (1996).
30. D. L. Windt, W. C. Cash, Jr., M. Scott, P. Arendt, B. Newnam, R. F. Fisher, A. B. Swartzlander, P. Z. Takacs, and J. M. Pinneo, *Appl. Opt.* **27**, 279 (1988).

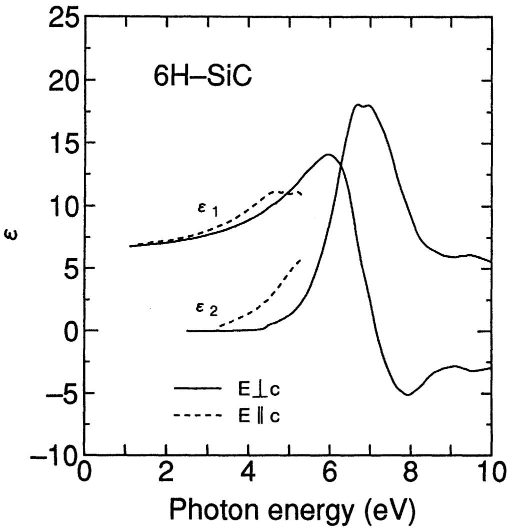


**Figure A6-5** $\varepsilon_1(E)$ and $\varepsilon_2(E)$ spectra for 6H-SiC at 300 K.

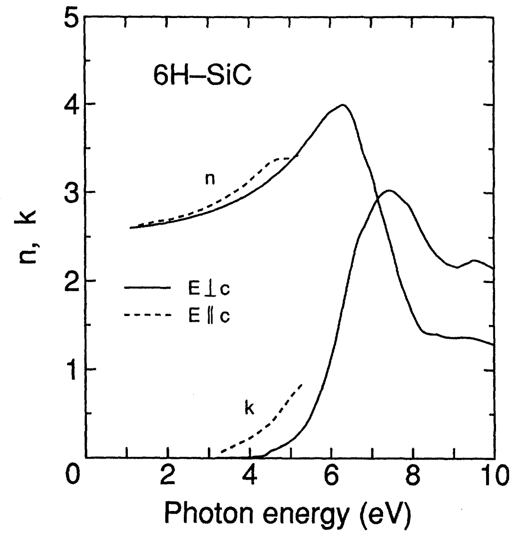


**Figure A6-6** $n(E)$ and $k(E)$ spectra for 6H-SiC at 300 K.

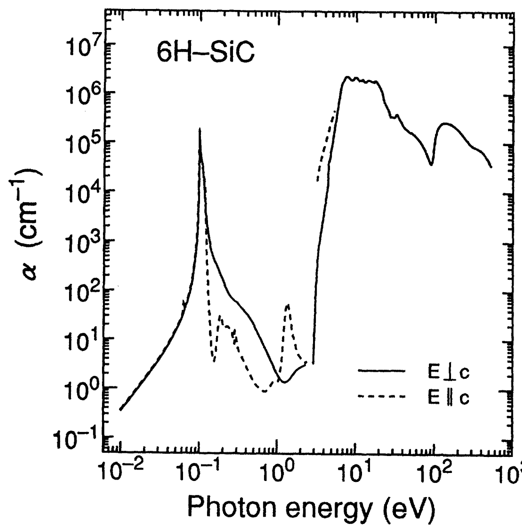


**Figure A6-7** $\alpha(E)$ spectra for 6H-SiC at 300 K.

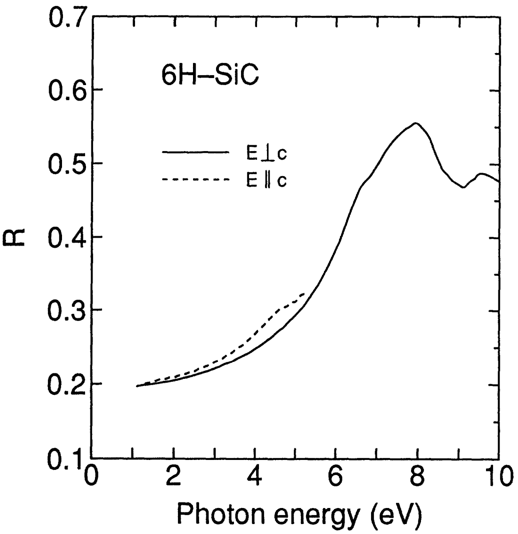


**Figure A6-8** *R*(*E*) spectra for 6H-SiC at 300 K.

**Table A6-4** *Optical constants of 6H-SiC for E⊥c at 300 K.*

| eV | $\varepsilon_1$ | $\varepsilon_2$ | *n* | *k* | $\alpha$ ($cm^{-1}$) | *R* |
|---|---|---|---|---|---|---|
| 0.01 | 9.164 | 0.0021 | 3.027 | 0.00034 | 3.49E-01 | 0.253 |
| 0.02 | 9.260 | 0.0044 | 3.043 | 0.00073 | 1.48E+00 | 0.255 |
| 0.03 | 9.435 | 0.0074 | 3.072 | 0.0012 | 3.68E+00 | 0.259 |
| 0.04 | 9.715 | 0.012 | 3.117 | 0.0019 | 7.59E+00 | 0.264 |
| 0.05 | 10.15 | 0.018 | 3.187 | 0.0029 | 1.47E+01 | 0.273 |
| 0.06 | 10.87 | 0.031 | 3.296 | 0.0047 | 2.84E+01 | 0.286 |
| 0.07 | 12.12 | 0.058 | 3.482 | 0.0083 | 5.87E+01 | 0.307 |
| 0.08 | 14.78 | 0.138 | 3.844 | 0.018 | 1.45E+02 | 0.345 |
| 0.09 | 23.58 | 0.634 | 4.856 | 0.065 | 5.96E+02 | 0.434 |
| 0.092 | 28.45 | 1.063 | 5.335 | 0.100 | 9.29E+02 | 0.468 |
| 0.094 | 37.36 | 2.133 | 6.114 | 0.174 | 1.66E+03 | 0.517 |
| 0.096 | 58.68 | 6.236 | 7.671 | 0.406 | 3.96E+03 | 0.593 |
| 0.098 | 164.2 | 67.07 | 13.07 | 2.566 | 2.55E+04 | 0.744 |
| 0.0982 | 194.7 | 107.3 | 14.44 | 3.717 | 3.70E+04 | 0.771 |
| 0.0984 | 222.6 | 186.9 | 16.02 | 5.834 | 5.82E+04 | 0.802 |
| 0.09844 | 224.7 | 210.5 | 16.32 | 6.449 | 6.44E+04 | 0.809 |
| 0.09848 | 224.0 | 237.0 | 16.58 | 7.146 | 7.13E+04 | 0.816 |
| 0.09852 | 219.3 | 266.6 | 16.80 | 7.935 | 7.93E+04 | 0.823 |
| 0.09856 | 209.3 | 298.7 | 16.94 | 8.816 | 8.81E+04 | 0.830 |
| 0.0986 | 192.4 | 332.2 | 16.98 | 9.785 | 9.78E+04 | 0.838 |
| 0.09864 | 167.4 | 365.3 | 16.87 | 10.83 | 1.08E+05 | 0.845 |
| 0.09868 | 133.5 | 395.3 | 16.59 | 11.91 | 1.19E+05 | 0.853 |
| 0.09872 | 91.19 | 418.9 | 16.12 | 12.99 | 1.30E+05 | 0.860 |
| 0.09876 | 42.47 | 432.9 | 15.45 | 14.01 | 1.40E+05 | 0.868 |
| 0.0988 | -9.181 | 435.2 | 14.60 | 14.91 | 1.49E+05 | 0.875 |
| 0.09884 | -59.50 | 425.5 | 13.60 | 15.64 | 1.57E+05 | 0.881 |
| 0.09888 | -104.6 | 405.2 | 12.53 | 16.17 | 1.62E+05 | 0.887 |

**Table A6-4** *Continued (6H-SiC, E⊥c).*

| eV | $\varepsilon_1$ | $\varepsilon_2$ | *n* | *k* | $\alpha$ (cm$^{-1}$) | *R* |
|---|---|---|---|---|---|---|
| 0.09892 | -141.8 | 377.2 | 11.43 | 16.50 | 1.66E+05 | 0.893 |
| 0.09896 | -170.2 | 344.9 | 10.36 | 16.66 | 1.67E+05 | 0.898 |
| 0.099 | -190.0 | 311.3 | 9.347 | 16.65 | 1.67E+05 | 0.903 |
| 0.09904 | -202.4 | 278.5 | 8.423 | 16.53 | 1.66E+05 | 0.907 |
| 0.09908 | -208.9 | 247.9 | 7.592 | 16.33 | 1.64E+05 | 0.911 |
| 0.0992 | -206.5 | 173.8 | 5.631 | 15.43 | 1.55E+05 | 0.920 |
| 0.0994 | -176.9 | 100.8 | 3.654 | 13.79 | 1.39E+05 | 0.931 |
| 0.0996 | -147.0 | 63.62 | 2.567 | 12.39 | 1.25E+05 | 0.938 |
| 0.0998 | -123.3 | 43.21 | 1.917 | 11.27 | 1.14E+05 | 0.943 |
| 0.1 | -105.2 | 31.06 | 1.498 | 10.37 | 1.05E+05 | 0.947 |
| 0.101 | -57.77 | 9.818 | 0.644 | 7.628 | 7.81E+04 | 0.958 |
| 0.105 | -16.61 | 1.269 | 0.156 | 4.078 | 4.34E+04 | 0.965 |
| 0.11 | -6.173 | 0.390 | 0.078 | 2.486 | 2.77E+04 | 0.957 |
| 0.12 | -0.060 | 0.108 | 0.178 | 0.303 | 3.69E+03 | 0.518 |
| 0.14 | 3.231 | 0.177 | 1.798 | 0.049 | 7.00E+02 | 0.082 |
| 0.16 | 4.344 | 0.098 | 2.084 | 0.023 | 3.80E+02 | 0.124 |
| 0.18 | 4.893 | 0.058 | 2.212 | 0.013 | 2.40E+02 | 0.142 |
| 0.2 | 5.214 | 0.036 | 2.283 | 0.0079 | 1.60E+02 | 0.153 |
| 0.22 | 5.422 | 0.023 | 2.328 | 0.0049 | 1.10E+02 | 0.159 |
| 0.24 | 5.565 | 0.016 | 2.359 | 0.0035 | 8.40E+01 | 0.164 |
| 0.26 | 5.670 | 0.013 | 2.381 | 0.0027 | 7.10E+01 | 0.167 |
| 0.28 | 5.749 | 0.011 | 2.398 | 0.0022 | 6.30E+01 | 0.169 |
| 0.3 | 5.810 | 0.0092 | 2.410 | 0.0019 | 5.80E+01 | 0.171 |
| 0.32 | 5.858 | 0.0076 | 2.420 | 0.0016 | 5.10E+01 | 0.172 |
| 0.34 | 5.897 | 0.0065 | 2.428 | 0.0013 | 4.64E+01 | 0.174 |
| 0.36 | 5.929 | 0.0056 | 2.435 | 0.0012 | 4.20E+01 | 0.175 |
| 0.38 | 5.955 | 0.0048 | 2.440 | 0.0010 | 3.75E+01 | 0.175 |
| 0.4 | 5.977 | 0.0041 | 2.445 | 8.43E-04 | 3.42E+01 | 0.176 |
| 0.42 | 5.996 | 0.0036 | 2.449 | 7.28E-04 | 3.10E+01 | 0.176 |
| 0.44 | 6.013 | 0.0031 | 2.452 | 6.28E-04 | 2.80E+01 | 0.177 |
| 0.46 | 6.027 | 0.0027 | 2.455 | 5.40E-04 | 2.52E+01 | 0.177 |
| 0.48 | 6.039 | 0.0023 | 2.457 | 4.69E-04 | 2.28E+01 | 0.178 |
| 0.5 | 6.050 | 0.0019 | 2.460 | 3.95E-04 | 2.00E+01 | 0.178 |
| 0.7 | 6.673 | 0.00049 | 2.583 | 9.44E-05 | 6.70E+00 | 0.195 |
| 0.9 | 6.706 | 0.00016 | 2.590 | 3.11E-05 | 2.84E+00 | 0.196 |
| 1.1 | 6.747 | 7.45E-05 | 2.598 | 1.43E-05 | 1.60E+00 | 0.197 |
| 1.3 | 6.798 | 5.58E-05 | 2.607 | 1.07E-05 | 1.41E+00 | 0.199 |
| 1.5 | 6.859 | 5.99E-05 | 2.619 | 1.14E-05 | 1.74E+00 | 0.200 |
| 1.7 | 6.930 | 6.96E-05 | 2.632 | 1.32E-05 | 2.28E+00 | 0.202 |
| 1.9 | 7.012 | 7.34E-05 | 2.648 | 1.39E-05 | 2.67E+00 | 0.204 |
| 2.1 | 7.105 | 7.39E-05 | 2.666 | 1.39E-05 | 2.95E+00 | 0.206 |
| 2.3 | 7.212 | 7.28E-05 | 2.685 | 1.36E-05 | 3.16E+00 | 0.209 |
| 2.5 | 7.332 | | 2.708 | | | 0.212 |
| 2.7 | 7.468 | | 2.733 | | | 0.215 |
| 2.9 | 7.622 | 6.20E-05 | 2.761 | 1.12E-05 | 3.30E+00 | 0.219 |
| 3 | 7.706 | 2.65E-04 | 2.776 | 4.77E-05 | 1.45E+01 | 0.221 |
| 3.1 | 7.795 | 0.0015 | 2.792 | 2.74E-04 | 8.60E+01 | 0.223 |
| 3.2 | 7.889 | 0.0045 | 2.809 | 8.01E-04 | 2.60E+02 | 0.226 |
| 3.3 | 7.989 | 0.0090 | 2.827 | 0.0016 | 5.30E+02 | 0.228 |
| 3.4 | 8.096 | 0.014 | 2.845 | 0.0024 | 8.40E+02 | 0.230 |

**Table A6-4** *Continued (6H-SiC, E⊥c).*

| eV | $\varepsilon_1$ | $\varepsilon_2$ | $n$ | $k$ | $\alpha$ (cm$^{-1}$) | $R$ |
|---|---|---|---|---|---|---|
| 3.5 | 8.209 | 0.019 | 2.865 | 0.0034 | 1.20E+03 | 0.233 |
| 3.6 | 8.330 | 0.025 | 2.886 | 0.0044 | 1.60E+03 | 0.236 |
| 3.7 | 8.458 | 0.032 | 2.908 | 0.0055 | 2.07E+03 | 0.238 |
| 3.8 | 8.595 | 0.041 | 2.932 | 0.0070 | 2.70E+03 | 0.241 |
| 3.9 | 8.730 | 0.052 | 2.955 | 0.0089 | 3.50E+03 | 0.244 |
| 4 | 8.897 | 0.068 | 2.983 | 0.011 | 4.60E+03 | 0.248 |
| 4.1 | 9.064 | 0.088 | 3.011 | 0.015 | 6.10E+03 | 0.251 |
| 4.2 | 9.242 | 0.120 | 3.040 | 0.020 | 8.40E+03 | 0.255 |
| 4.3 | 9.433 | 0.155 | 3.071 | 0.025 | 1.10E+04 | 0.259 |
| 4.4 | 9.639 | 0.195 | 3.105 | 0.031 | 1.40E+04 | 0.263 |
| 4.5 | 9.925 | 0.535 | 3.140 | 0.085 | 3.87E+04 | 0.268 |
| 4.6 | 10.16 | 0.599 | 3.189 | 0.094 | 4.38E+04 | 0.273 |
| 4.7 | 10.31 | 0.727 | 3.213 | 0.113 | 5.39E+04 | 0.276 |
| 4.8 | 10.62 | 0.941 | 3.262 | 0.144 | 7.02E+04 | 0.283 |
| 4.9 | 10.91 | 1.070 | 3.307 | 0.162 | 8.03E+04 | 0.288 |
| 5 | 11.18 | 1.305 | 3.349 | 0.195 | 9.88E+04 | 0.293 |
| 5.1 | 11.49 | 1.540 | 3.397 | 0.227 | 1.17E+05 | 0.299 |
| 5.2 | 11.81 | 1.882 | 3.447 | 0.273 | 1.44E+05 | 0.305 |
| 5.3 | 12.21 | 2.310 | 3.510 | 0.329 | 1.77E+05 | 0.313 |
| 5.4 | 12.64 | 2.781 | 3.577 | 0.389 | 2.13E+05 | 0.322 |
| 5.5 | 12.94 | 3.422 | 3.628 | 0.472 | 2.63E+05 | 0.329 |
| 5.6 | 13.24 | 4.278 | 3.685 | 0.581 | 3.30E+05 | 0.339 |
| 5.7 | 13.60 | 5.134 | 3.751 | 0.684 | 3.95E+05 | 0.349 |
| 5.8 | 13.88 | 6.203 | 3.814 | 0.813 | 4.78E+05 | 0.360 |
| 5.9 | 14.11 | 7.412 | 3.876 | 0.956 | 5.72E+05 | 0.372 |
| 6 | 14.12 | 8.770 | 3.920 | 1.119 | 6.80E+05 | 0.384 |
| 6.1 | 13.93 | 10.16 | 3.947 | 1.287 | 7.96E+05 | 0.396 |
| 6.2 | 13.52 | 11.98 | 3.974 | 1.507 | 9.47E+05 | 0.412 |
| 6.3 | 13.10 | 13.80 | 4.008 | 1.721 | 1.10E+06 | 0.428 |
| 6.4 | 12.09 | 15.38 | 3.978 | 1.933 | 1.25E+06 | 0.442 |
| 6.5 | 10.70 | 16.86 | 3.915 | 2.153 | 1.42E+06 | 0.456 |
| 6.6 | 8.834 | 17.97 | 3.798 | 2.365 | 1.58E+06 | 0.469 |
| 6.7 | 6.759 | 18.18 | 3.616 | 2.514 | 1.71E+06 | 0.476 |
| 6.8 | 5.155 | 17.86 | 3.446 | 2.592 | 1.79E+06 | 0.480 |
| 6.9 | 3.850 | 18.02 | 3.338 | 2.700 | 1.89E+06 | 0.489 |
| 7 | 2.567 | 18.07 | 3.227 | 2.801 | 1.99E+06 | 0.498 |
| 7.1 | 0.802 | 17.56 | 3.032 | 2.896 | 2.08E+06 | 0.508 |
| 7.2 | -0.684 | 16.86 | 2.845 | 2.963 | 2.16E+06 | 0.517 |
| 7.3 | -1.765 | 16.17 | 2.693 | 3.003 | 2.22E+06 | 0.525 |
| 7.4 | -2.727 | 15.36 | 2.537 | 3.027 | 2.27E+06 | 0.532 |
| 7.5 | -3.551 | 14.33 | 2.368 | 3.026 | 2.30E+06 | 0.538 |
| 7.6 | -4.225 | 13.05 | 2.178 | 2.995 | 2.31E+06 | 0.543 |
| 7.7 | -4.706 | 11.82 | 2.002 | 2.952 | 2.30E+06 | 0.548 |
| 7.8 | -4.888 | 10.93 | 1.882 | 2.904 | 2.30E+06 | 0.550 |
| 7.9 | -5.155 | 10.12 | 1.761 | 2.873 | 2.30E+06 | 0.556 |
| 8 | -5.091 | 9.176 | 1.644 | 2.792 | 2.26E+06 | 0.555 |
| 8.1 | -4.813 | 8.321 | 1.549 | 2.686 | 2.21E+06 | 0.548 |
| 8.2 | -4.599 | 7.540 | 1.455 | 2.591 | 2.15E+06 | 0.543 |
| 8.3 | -4.278 | 7.102 | 1.416 | 2.507 | 2.11E+06 | 0.533 |
| 8.4 | -3.850 | 6.781 | 1.405 | 2.413 | 2.06E+06 | 0.516 |

**Table A6-4** *Continued (6H-SiC, $E\perp c$).*

| eV | $\varepsilon_1$ | $\varepsilon_2$ | *n* | *k* | $\alpha$ (cm$^{-1}$) | *R* |
|---|---|---|---|---|---|---|
| 8.5 | -3.561 | 6.578 | 1.400 | 2.350 | 2.02E+06 | 0.504 |
| 8.6 | -3.262 | 6.417 | 1.403 | 2.287 | 1.99E+06 | 0.490 |
| 8.7 | -3.187 | 6.225 | 1.379 | 2.256 | 1.99E+06 | 0.487 |
| 8.8 | -2.995 | 6.053 | 1.371 | 2.208 | 1.97E+06 | 0.478 |
| 8.9 | -2.941 | 5.989 | 1.366 | 2.192 | 1.98E+06 | 0.475 |
| 9 | -2.888 | 5.936 | 1.363 | 2.178 | 1.99E+06 | 0.472 |
| 9.1 | -2.781 | 5.882 | 1.365 | 2.155 | 1.99E+06 | 0.467 |
| 9.2 | -2.888 | 5.979 | 1.370 | 2.183 | 2.04E+06 | 0.472 |
| 9.3 | -2.995 | 6.011 | 1.364 | 2.203 | 2.08E+06 | 0.478 |
| 9.4 | -3.027 | 6.043 | 1.366 | 2.212 | 2.11E+06 | 0.479 |
| 9.5 | -3.316 | 6.171 | 1.358 | 2.272 | 2.19E+06 | 0.493 |
| 10.2 | -2.822 | 5.292 | 1.26 | 2.10 | 2.17E+06 | 0.470 |
| 10.3 | -2.673 | 4.978 | 1.22 | 2.04 | 2.14E+06 | 0.463 |
| 10.8 | -2.180 | 3.372 | 0.958 | 1.76 | 1.92E+06 | 0.447 |
| 11.4 | -1.907 | 3.292 | 0.974 | 1.69 | 1.96E+06 | 0.423 |
| 11.6 | -1.890 | 2.777 | 0.857 | 1.62 | 1.91E+06 | 0.436 |
| 11.8 | -1.867 | 2.898 | 0.889 | 1.63 | 1.95E+06 | 0.429 |
| 12.1 | -1.723 | 3.300 | 1.00 | 1.65 | 2.02E+06 | 0.405 |
| 12.5 | -1.418 | 2.534 | 0.862 | 1.47 | 1.87E+06 | 0.387 |
| 13.3 | -1.200 | 2.006 | 0.754 | 1.33 | 1.79E+06 | 0.378 |
| 13.5 | -1.254 | 2.162 | 0.789 | 1.37 | 1.87E+06 | 0.378 |
| 14.1 | -1.219 | 2.222 | 0.811 | 1.37 | 1.96E+06 | 0.371 |
| 14.9 | -1.096 | 1.826 | 0.719 | 1.27 | 1.91E+06 | 0.370 |
| 16.7 | -0.779 | 1.244 | 0.587 | 1.06 | 1.79E+06 | 0.355 |
| 16.8 | -0.793 | 1.269 | 0.593 | 1.07 | 1.83E+06 | 0.356 |
| 17.3 | -0.872 | 1.225 | 0.562 | 1.09 | 1.91E+06 | 0.380 |
| 18.5 | -0.593 | 0.935 | 0.507 | 0.922 | 1.73E+06 | 0.350 |
| 20.1 | -0.264 | 0.576 | 0.430 | 0.670 | 1.37E+06 | 0.310 |
| 21.2 | -0.110 | 0.417 | 0.401 | 0.520 | 1.12E+06 | 0.282 |
| 23 | 0.159 | 0.279 | 0.490 | 0.285 | 6.64E+05 | 0.148 |
| 25.3 | 0.330 | 0.234 | 0.606 | 0.193 | 4.95E+05 | 0.074 |
| 26.9 | 0.424 | 0.173 | 0.664 | 0.130 | 3.55E+05 | 0.047 |
| 27.7 | 0.458 | 0.171 | 0.688 | 0.124 | 3.48E+05 | 0.039 |
| 30.5 | 0.556 | 0.166 | 0.754 | 0.110 | 3.41E+05 | 0.024 |
| 32.7 | 0.588 | 0.182 | 0.776 | 0.117 | 3.88E+05 | 0.020 |
| 34.7 | 0.627 | 0.145 | 0.797 | 0.0909 | 3.20E+05 | 0.015 |
| 37.9 | 0.673 | 0.110 | 0.823 | 0.0668 | 2.57E+05 | 0.011 |
| 40.8 | 0.727 | 0.087 | 0.854 | 0.0511 | 2.11E+05 | 6.96E-03 |
| 48.4 | 0.786 | 0.060 | 0.887 | 0.0339 | 1.66E+05 | 3.91E-03 |
| 51 | 0.796 | 0.056 | 0.893 | 0.0315 | 1.63E+05 | 3.47E-03 |
| 72.3 | 0.911 | 0.021 | 0.9547 | 0.0110 | 8.06E+04 | 5.69E-04 |
| 91.5 | 0.959 | 0.008 | 0.9791 | 0.0043 | 4.02E+04 | 1.16E-04 |
| 108.7 | 0.973 | 0.036 | 0.9866 | 0.0181 | 2.00E+05 | 1.28E-04 |
| 183.4 | 0.970 | 0.022 | 0.9851 | 0.0114 | 2.12E+05 | 8.93E-05 |
| 277.3 | 0.988 | 0.0069 | 0.99387 | 3.46E-03 | 9.73E+04 | 1.25E-05 |
| 392.2 | 0.992 | 0.0035 | 0.99579 | 1.74E-03 | 6.92E+04 | 5.21E-06 |
| 525.2 | 0.995 | 0.0013 | 0.99733 | 6.58E-04 | 3.50E+04 | 1.90E-06 |

**Table A6-5** *Optical constants of 6H-SiC for E||c at 300 K.*

| eV | $\varepsilon_1$ | $\varepsilon_2$ | $n$ | $k$ | $\alpha$ (cm$^{-1}$) | $R$ |
|---|---|---|---|---|---|---|
| 0.01 | 9.755 | 2.30E-03 | 3.123 | 3.68E-04 | 3.73E-01 | 0.265 |
| 0.02 | 9.863 | 4.90E-03 | 3.140 | 7.80E-04 | 1.58E+00 | 0.267 |
| 0.03 | 10.06 | 8.23E-03 | 3.171 | 1.30E-03 | 3.95E+00 | 0.271 |
| 0.04 | 10.37 | 0.013 | 3.221 | 2.02E-03 | 8.18E+00 | 0.277 |
| 0.05 | 10.87 | 0.021 | 3.297 | 3.13E-03 | 1.59E+01 | 0.286 |
| 0.06 | 11.68 | 0.035 | 3.418 | 5.15E-03 | 3.13E+01 | 0.300 |
| 0.062 | 11.91 | 0.046 | 3.451 | 6.71E-03 | 4.22E+01 | 0.303 |
| 0.0622 | 11.94 | 0.052 | 3.455 | 7.59E-03 | 4.78E+01 | 0.304 |
| 0.0624 | 11.95 | 0.060 | 3.457 | 8.75E-03 | 5.53E+01 | 0.304 |
| 0.0626 | 11.97 | 0.060 | 3.459 | 8.69E-03 | 5.51E+01 | 0.304 |
| 0.0628 | 11.99 | 0.055 | 3.462 | 7.93E-03 | 5.05E+01 | 0.305 |
| 0.063 | 12.01 | 0.052 | 3.466 | 7.49E-03 | 4.78E+01 | 0.305 |
| 0.0632 | 12.04 | 0.049 | 3.469 | 7.01E-03 | 4.49E+01 | 0.305 |
| 0.0634 | 12.06 | 0.047 | 3.473 | 6.71E-03 | 4.31E+01 | 0.306 |
| 0.07 | 13.13 | 0.067 | 3.624 | 9.19E-03 | 6.52E+01 | 0.322 |
| 0.08 | 16.30 | 0.166 | 4.037 | 0.021 | 1.67E+02 | 0.364 |
| 0.09 | 27.85 | 0.886 | 5.278 | 0.084 | 7.66E+02 | 0.464 |
| 0.092 | 35.03 | 1.620 | 5.920 | 0.137 | 1.28E+03 | 0.506 |
| 0.094 | 49.90 | 3.849 | 7.069 | 0.272 | 2.59E+03 | 0.566 |
| 0.096 | 98.01 | 18.01 | 9.941 | 0.906 | 8.82E+03 | 0.670 |
| 0.0964 | 123.3 | 30.28 | 11.187 | 1.353 | 1.32E+04 | 0.702 |
| 0.0968 | 165.2 | 60.11 | 13.056 | 2.302 | 2.26E+04 | 0.743 |
| 0.097 | 195.8 | 93.15 | 14.364 | 3.242 | 3.19E+04 | 0.767 |
| 0.0972 | 230.7 | 157.1 | 15.965 | 4.921 | 4.85E+04 | 0.795 |
| 0.0974 | 240.0 | 284.0 | 17.490 | 8.120 | 8.02E+04 | 0.828 |
| 0.0975 | 201.2 | 374.2 | 17.692 | 10.58 | 1.05E+05 | 0.847 |
| 0.0976 | 105.6 | 453.3 | 16.898 | 13.41 | 1.33E+05 | 0.865 |
| 0.0977 | -32.37 | 471.3 | 14.833 | 15.89 | 1.57E+05 | 0.882 |
| 0.0978 | -151.9 | 413.3 | 12.008 | 17.21 | 1.71E+05 | 0.897 |
| 0.098 | -230.0 | 240.3 | 7.163 | 16.77 | 1.67E+05 | 0.918 |
| 0.0982 | -206.6 | 134.5 | 4.469 | 15.05 | 1.50E+05 | 0.930 |
| 0.0984 | -171.9 | 81.76 | 3.037 | 13.46 | 1.34E+05 | 0.938 |
| 0.0988 | -121.3 | 37.86 | 1.699 | 11.14 | 1.12E+05 | 0.948 |
| 0.0992 | -91.19 | 21.41 | 1.113 | 9.614 | 9.67E+04 | 0.954 |
| 0.0996 | -72.09 | 13.68 | 0.802 | 8.528 | 8.61E+04 | 0.958 |
| 0.1 | -59.05 | 9.465 | 0.614 | 7.709 | 7.82E+04 | 0.960 |
| 0.102 | -28.90 | 2.778 | 0.258 | 5.382 | 5.57E+04 | 0.966 |
| 0.104 | -17.53 | 1.304 | 0.156 | 4.190 | 4.42E+04 | 0.967 |
| 0.106 | -11.58 | 0.757 | 0.111 | 3.405 | 3.66E+04 | 0.965 |
| 0.108 | -7.880 | 0.510 | 0.091 | 2.809 | 3.08E+04 | 0.960 |
| 0.1086 | -6.996 | 0.487 | 0.092 | 2.647 | 2.91E+04 | 0.955 |
| 0.1088 | -6.710 | 0.494 | 0.095 | 2.592 | 2.86E+04 | 0.952 |
| 0.109 | -6.427 | 0.522 | 0.103 | 2.537 | 2.80E+04 | 0.946 |
| 0.1092 | -6.155 | 0.591 | 0.119 | 2.484 | 2.75E+04 | 0.936 |
| 0.1094 | -5.954 | 0.725 | 0.148 | 2.445 | 2.71E+04 | 0.919 |
| 0.1095 | -5.918 | 0.787 | 0.161 | 2.438 | 2.71E+04 | 0.912 |
| 0.1096 | -5.913 | 0.798 | 0.164 | 2.437 | 2.71E+04 | 0.910 |
| 0.1097 | -5.888 | 0.755 | 0.155 | 2.432 | 2.70E+04 | 0.914 |
| 0.1098 | -5.821 | 0.699 | 0.145 | 2.417 | 2.69E+04 | 0.919 |
| 0.11 | -5.636 | 0.645 | 0.136 | 2.378 | 2.65E+04 | 0.922 |

**Table A6-5** *Continued (6H-SiC, E||c).*

| eV | $\varepsilon_1$ | $\varepsilon_2$ | *n* | *k* | $\alpha$ (cm$^{-1}$) | *R* |
|---|---|---|---|---|---|---|
| 0.1102 | -5.507 | 0.607 | 0.129 | 2.350 | 2.63E+04 | 0.924 |
| 0.1104 | -5.353 | 0.501 | 0.108 | 2.316 | 2.59E+04 | 0.934 |
| 0.1106 | -5.142 | 0.418 | 0.092 | 2.270 | 2.54E+04 | 0.942 |
| 0.1108 | -4.928 | 0.369 | 0.083 | 2.221 | 2.50E+04 | 0.946 |
| 0.111 | -4.724 | 0.339 | 0.078 | 2.175 | 2.45E+04 | 0.947 |
| 0.1112 | -4.530 | 0.318 | 0.075 | 2.130 | 2.40E+04 | 0.948 |
| 0.112 | -3.838 | 0.267 | 0.068 | 1.960 | 2.23E+04 | 0.945 |
| 0.114 | -2.459 | 0.199 | 0.063 | 1.569 | 1.81E+04 | 0.930 |
| 0.116 | -1.399 | 0.156 | 0.066 | 1.185 | 1.39E+04 | 0.896 |
| 0.118 | -0.553 | 0.126 | 0.084 | 0.749 | 8.96E+03 | 0.805 |
| 0.12 | 0.138 | 0.104 | 0.395 | 0.132 | 1.61E+03 | 0.195 |
| 0.14 | 3.424 | 2.84E-03 | 1.850 | 7.66E-04 | 1.09E+01 | 0.089 |
| 0.16 | 4.570 | 1.27E-03 | 2.138 | 2.97E-04 | 4.82E+00 | 0.131 |
| 0.18 | 5.141 | 7.06E-03 | 2.267 | 1.56E-03 | 2.84E+01 | 0.150 |
| 0.2 | 5.478 | 4.42E-03 | 2.340 | 9.43E-04 | 1.91E+01 | 0.161 |
| 0.22 | 5.697 | 3.95E-03 | 2.387 | 8.27E-04 | 1.85E+01 | 0.168 |
| 0.24 | 5.847 | 3.48E-03 | 2.418 | 7.19E-04 | 1.75E+01 | 0.172 |
| 0.26 | 5.959 | 2.61E-03 | 2.441 | 5.35E-04 | 1.41E+01 | 0.175 |
| 0.28 | 6.042 | 1.44E-03 | 2.458 | 2.92E-04 | 8.30E+00 | 0.178 |
| 0.282 | 6.055 | 2.58E-03 | 2.461 | 5.25E-04 | 1.50E+01 | 0.178 |
| 0.3 | 6.107 | 1.48E-03 | 2.471 | 2.99E-04 | 9.10E+00 | 0.180 |
| 0.32 | 6.158 | 8.72E-04 | 2.482 | 1.76E-04 | 5.70E+00 | 0.181 |
| 0.34 | 6.199 | 6.93E-04 | 2.490 | 1.39E-04 | 4.80E+00 | 0.182 |
| 0.36 | 6.233 | 5.47E-04 | 2.497 | 1.10E-04 | 4.00E+00 | 0.183 |
| 0.38 | 6.261 | 4.42E-04 | 2.502 | 8.83E-05 | 3.40E+00 | 0.184 |
| 0.4 | 6.285 | 3.46E-04 | 2.507 | 6.90E-05 | 2.80E+00 | 0.185 |
| 0.42 | 6.305 | 2.89E-04 | 2.511 | 5.75E-05 | 2.45E+00 | 0.185 |
| 0.44 | 6.322 | 2.40E-04 | 2.514 | 4.77E-05 | 2.13E+00 | 0.186 |
| 0.46 | 6.337 | 1.98E-04 | 2.517 | 3.92E-05 | 1.83E+00 | 0.186 |
| 0.48 | 6.350 | 1.64E-04 | 2.520 | 3.25E-05 | 1.58E+00 | 0.186 |
| 0.5 | 6.362 | 1.39E-04 | 2.522 | 2.76E-05 | 1.40E+00 | 0.187 |
| 0.7 | 6.530 | 6.48E-05 | 2.555 | 1.27E-05 | 9.00E-01 | 0.191 |
| 0.9 | 6.670 | 7.87E-05 | 2.583 | 1.52E-05 | 1.39E+00 | 0.195 |
| 1.1 | 6.790 | 1.08E-04 | 2.606 | 2.07E-05 | 2.31E+00 | 0.198 |
| 1.3 | 6.89 | 1.95E-03 | 2.625 | 3.72E-04 | 4.90E+01 | 0.201 |
| 1.5 | 6.98 | 7.68E-04 | 2.643 | 1.45E-04 | 2.21E+01 | 0.203 |
| 1.7 | 7.11 | 2.60E-04 | 2.666 | 4.87E-05 | 8.40E+00 | 0.207 |
| 1.8 | 7.14 | 1.67E-04 | 2.672 | 3.12E-05 | 5.70E+00 | 0.207 |
| 1.9 | 7.21 | 1.37E-04 | 2.686 | 2.54E-05 | 4.90E+00 | 0.209 |
| 2 | 7.20 | 1.16E-04 | 2.684 | 2.17E-05 | 4.40E+00 | 0.209 |
| 2.1 | 7.27 | 9.88E-05 | 2.697 | 1.83E-05 | 3.90E+00 | 0.211 |
| 2.2 | 7.34 | 8.82E-05 | 2.710 | 1.63E-05 | 3.63E+00 | 0.212 |
| 2.3 | 7.41 | 8.17E-05 | 2.723 | 1.50E-05 | 3.50E+00 | 0.214 |
| 2.4 | 7.47 | 8.16E-05 | 2.734 | 1.49E-05 | 3.63E+00 | 0.216 |
| 2.5 | 7.54 | | 2.747 | | | 0.217 |
| 2.6 | 7.64 | | 2.763 | | | 0.220 |
| 2.7 | 7.74 | | 2.782 | | | 0.222 |
| 2.8 | 7.83 | | 2.798 | | | 0.224 |
| 2.9 | 7.94 | | 2.817 | | | 0.227 |
| 3 | 8.06 | | 2.840 | | | 0.230 |

**Table A6-5** *Continued (6H-SiC, E||c).*

| eV | $\varepsilon_1$ | $\varepsilon_2$ | $n$ | $k$ | $\alpha$ (cm$^{-1}$) | $R$ |
|---|---|---|---|---|---|---|
| 3.1 | 8.18 | | 2.860 | | | 0.232 |
| 3.2 | 8.32 | 0.3 | 2.884 | 0.052 | 1.69E+04 | 0.235 |
| 3.3 | 8.46 | 0.4 | 2.909 | 0.069 | 2.30E+04 | 0.239 |
| 3.4 | 8.61 | 0.52 | 2.936 | 0.089 | 3.05E+04 | 0.242 |
| 3.5 | 8.76 | 0.66 | 2.962 | 0.111 | 3.95E+04 | 0.246 |
| 3.6 | 8.92 | 0.79 | 2.990 | 0.132 | 4.82E+04 | 0.250 |
| 3.7 | 9.09 | 0.95 | 3.019 | 0.157 | 5.90E+04 | 0.253 |
| 3.8 | 9.31 | 1.09 | 3.056 | 0.178 | 6.87E+04 | 0.258 |
| 3.9 | 9.50 | 1.23 | 3.088 | 0.199 | 7.87E+04 | 0.263 |
| 4 | 9.74 | 1.41 | 3.130 | 0.225 | 9.14E+04 | 0.268 |
| 4.1 | 10.00 | 1.60 | 3.172 | 0.252 | 1.05E+05 | 0.274 |
| 4.2 | 10.23 | 1.79 | 3.210 | 0.279 | 1.19E+05 | 0.279 |
| 4.3 | 10.49 | 2.10 | 3.255 | 0.323 | 1.41E+05 | 0.285 |
| 4.4 | 10.74 | 2.36 | 3.296 | 0.358 | 1.60E+05 | 0.291 |
| 4.5 | 10.99 | 2.57 | 3.337 | 0.385 | 1.76E+05 | 0.296 |
| 4.6 | 11.11 | 3.00 | 3.362 | 0.446 | 2.08E+05 | 0.301 |
| 4.7 | 11.17 | 3.38 | 3.380 | 0.500 | 2.38E+05 | 0.304 |
| 4.8 | 11.08 | 3.81 | 3.376 | 0.564 | 2.75E+05 | 0.306 |
| 4.9 | 11.15 | 4.26 | 3.397 | 0.627 | 3.11E+05 | 0.311 |
| 5 | 10.95 | 4.65 | 3.380 | 0.688 | 3.49E+05 | 0.312 |
| 5.1 | 11.09 | 5.10 | 3.413 | 0.747 | 3.86E+05 | 0.319 |
| 5.2 | 11.13 | 5.42 | 3.428 | 0.790 | 4.17E+05 | 0.322 |
| 5.3 | 10.91 | 5.76 | 3.409 | 0.845 | 4.54E+05 | 0.323 |